Journal of Catalysis 258 (2008) 87–94

Contents lists available at ScienceDirect

Journal of Catalysis

www.elsevier.com/locate/jcat

Sulphuric acid and Pt treatment of the photocatalytically active titanium dioxide

D.V. Kozlov *, A.V. Vorontsov

Boreskov Institute of Catalysis and Novosibirsk State University, Novosibirsk 630090, Russian Federation

ARTICLE INFO

Article history:
Received 31 March 2008
Revised 26 May 2008
Accepted 30 May 2008
Available online 30 June 2008

Keywords:
Titanium dioxide
Gas phase photocatalytic oxidation
Surface acidity
Low temperature CO adsorption
Surface titration

ABSTRACT

The study focuses on preparation, surface sites characterization and catalytic activity testing of pure (TiO_2), sulfated (TiO_2-S), loaded with 1 wt% Pt (TiO_2-Pt) and platinized/sulfated (TiO_2-Pt-S) high surface area anatase TiO_2 (100% anatase, 340 m^2/g). Sulfation was performed in 4 M H_2SO_4 solution and was not followed by a high temperature calcination. TEM images reveal the formation of a 3 Å amorphous layer over TiO_2 and TiO_2-Pt surface after their sulfation. Infrared spectrum of TiO_2-S contains additional absorption bands at 1235, 1333 and 1378 cm^{-1} that are assigned to S=O stretch and distorted adsorbed SO_4^{2-} vibrations. Low temperature CO adsorption and organic species adsorption from heptane solutions was performed for characterization of surface sites. TiO_2-S showed 3–5 cm^{-1} shift of adsorbed CO absorption band compared to initial TiO_2. The quantity of adsorbed CO increased by a factor of 1.5 for TiO_2-S indicating the increase of the quantity of surface Lewis sites. Sulfation also resulted in disappearance of OH groups having absorption band at 3690 cm^{-1} that was attributed to substitution by monodentate and bidentate sulfates. Four bases and two acids with different pK were used as probes in solution titration revealing that the quantity of different acid sites in TiO_2-S increases 1.07–2.17 times. Unexpectedly the quantity of acid and base sites in TiO_2-Pt-S decreases relatively to other catalysts studied.

Catalytic activity of the samples in acetone deep photooxidation was measured as a function of acetone vapor concentration in a flow-circulating reactor. All dependences are well described by the one site Langmuir–Hinshelwood kinetic model. The maximum oxidation rate was similar for all samples and was observed at acetone concentration above 1500 ppm. However, in the range of low acetone concentration the activity of TiO_2-Pt-S was about triple of pure TiO_2 activity. The high activity of sulfated/platinized and sulfated TiO_2 is due to the much increased acetone adsorption constant.

1. Introduction

The sulfation of titanium dioxide was recently acknowledged as a way of enhancing its catalytic and photocatalytic activity. Reputable companies like Sachtleben Chemie GmbH are producing titanium dioxide containing several percent of sulfur in the form of sulfates for catalytic applications. Two companies in Russia which are producing photocatalytic air cleaners already use only sulfated TiO_2 because it demonstrates higher photocatalytic oxidation (PCO) rates for a variety of organic compounds. At the same time, the nature of PCO rates increase if any is still under active investigation and discussed by many researchers.

The evolution of understanding of the influence of TiO_2 acidic properties on its (photo)catalytic activity started from the 80's of the last century when researchers [1,2] had demonstrated the role of the number of hydroxyl groups on the oxygen photoadsorption. Later Papp et al. [3] measured the number of TiO_2 (Degussa P25 annealed at different temperatures) surface hydroxyl groups by the *n*-butylamine titration method [4] and revealed the correlation between this number and the rate of 1,4-dichlorobenzene photocatalytic oxidation in water solution. Kwon et al. [5] obtained the similar result with the WO_3/TiO_2 photocatalyst in the same reaction. Authors supposed that the increased surface acidity and therefore increased TiO_2 adsorption affinity was the main factor responsible for the photocatalytic activity increase.

Kantoh and Okazaki [6] investigated TiO_2 samples prepared from titanium tetraisopropoxide and $TiOSO_4$. The TiO_2 sample prepared from $TiOSO_4$ had both types of acid sites—Brønsted and Lewis, the later ones being converted into the Brønsted sites after addition of water due to the bidentate sulfate –Ti–O–SO_2–O–Ti– reaction. They also revealed the correlation between the amount of surface OH groups and the amount of reacting aminoalcohols in the autoclave.

Closely to the TiO_2 sulfation treatment, Deng et al. [7] prepared several TiO_2 samples using the sol–gel method and treated some of them with H_2SO_4. They demonstrated that the sulfated samples had a higher conversion and stability during the gas phase photocatalytic oxidation of hexane, benzene and methanol. The authors

* Corresponding author.
E-mail address: kdv@catalysis.ru (D.V. Kozlov).

0021-9517/$ – see front matter
doi:10.1016/j.jcat.2008.05.030

explained such behavior by the two simultaneous trends: the increase of the surface area of sulfated samples and the increase of their surface acidity. The first reason was the main according to the authors.

Colon et al. [8] also demonstrated that sulfated TiO_2 annealed at 600–700 °C had a higher photocatalytic activity in the water phase phenol PCO than pure TiO_2. The SO_4^{2-} ions were almost absent after the high temperature treatment. The authors attributed this effect to the TiO_2 surface stabilization by sulfates during the annealing and keeping a higher specific surface area compared with the pure untreated TiO_2. In their later work [9] the authors developed their previous conclusions and stated that the annealing of the sulfated samples leads to the creation of bulk oxygen vacancies through the dehydroxylation of the excess of adsorbed water giving a highly defective photocatalyst. It gives an enhancement of the PCO activity due to the improvement of the charge separation and diffusion to the surface. In their most recent work [10] these researchers conducted simultaneous TiO_2 sulfation and Pt deposition and demonstrated that the samples obtained are more active in the phenol PCO in water. The authors make the reasonable guess that the Pt deposition is affected by the preliminary sulfation giving the higher dispersion of obtained Pt particles. Other researchers [11] also attributed the improved activity of SO_4^{2-}/TiO_2 to the surface area increase.

Keller et al. [12,13] observed higher time on stream stability of sulfated sol–gel TiO_2 in gaseous toluene photocatalytic oxidation. Higher concentrations of H_2SO_4 resulted in higher photocatalytic activities. They attributed the enhanced stability to a lower adsorption of toluene over the catalyst surface and possible increased electron–hole pares separation. Muggli and Ding [14], on the contrary, observed higher adsorption of gaseous organic compounds. They also registered increased catalytic stability of sulfated TiO_2 compared to unsulfated one. As in the previously mentioned works, these authors used high temperature calcination after the H_2SO_4 treatment.

Yu with co-workers [15] suggested that the promoting effect of sulphuric acid is explained by the removal of sodium ion impurities from the glass used as a support during the TiO_2 thin films preparation.

Results which were cited above could not explain the enhanced photocatalytic activity of photocatalyst obtained by mild H_2SO_4 treatment with consequent washing and drying at a low (less than 150 °C) temperature since such SO_4^{2-}/TiO_2 samples contain much higher quantity of surface sulfates. In this case, the chemical and physico-chemical interactions of photocatalytic reaction substrates, products and intermediates should be taken into account. We had focused on such an approach in our previous research [16–18].

Platinum deposition has been used for a long time to enhance photocatalytic reactions over TiO_2 in liquid and gas phase [19–28]. Therefore, addition of Pt combined with sulfation is expected to provide further increase of TiO_2 photocatalytic activity. This opportunity was not investigated before for gas phase reactions. Moreover, platinum deposition over some kinds of TiO_2 can produce photocatalysts with decreased activity in gas phase reactions [29]. Of special interest is the capability of sulfuric acid treatment to improve the performance of these platinized TiO_2 samples.

In the present work, we employ the combination of platinum deposition and sulfation without subsequent high-temperature treatment in order to increase TiO_2 photocatalytic activity. The tandem of solution titration and CO adsorption methods is harnessed for characterization of TiO_2 surface acidity measurements, which is complemented by HR-TEM images of the catalyst surface.

Kinetic study on the acetone photocatalytic oxidation in a flow-circulating reactor reveals that sulfation of platinized TiO_2 results in strong increase of acetone adsorption constant that provides highly increased oxidation rate at the low acetone concentration while unmodified TiO_2 outperforms at the high acetone concentrations.

Table 1
Specific surface area, Pt and S content for TiO_2, TiO_2-S and TiO_2-Pt-S samples

Sample	S_{BET}, m^2/g	Pt content, wt%	S content, wt%
TiO_2	341	–	–
TiO_2-S	335	–	1.54
TiO_2-Pt-S	–	0.95	1.45

2. Experimental

2.1. Materials and catalyst preparation

Titanium dioxide Hombifine N (Sachtleben Chemie GmbH, 100% anatase, specific surface area 341 m^2/g) was used as supplied. H_2SO_4 (high-purity grade), $H_2PtCl_6{\cdot}6H_2O$ (38.12 wt% Pt) were used for TiO_2 modification. Deionized water from a Barnsted EASYpure II ultrapure water system was used for solutions preparation and photocatalysts treatment.

The TiO_2 sulfation method was described previously [17] and was used here with a minor modification. A 1 g TiO_2 sample was placed into a round-bottomed 100 ml flask; 50 ml of the 4 M H_2SO_4 aqueous solution was added. Then the flask was put into a thermostat and kept at 50 °C for 2 h under continuous stirring. Treated sample was then washed 6–7 times with deionized water with subsequent centrifugation. The amount of sulfates in the wash water was qualitatively controlled with a 1 M $BaCl_2$ solution. The prepared samples were finally dried in air at 120 °C for 2–3 h. Untreated initial TiO_2 sample and the sample modified with H_2SO_4 are referred to further in the text as TiO_2 and TiO_2-S, correspondingly.

To investigate the influence of Pt addition, a sample was prepared by the $NaBH_4$ reduction of adsorbed H_2PtCl_6. This sample is referred to as TiO_2-Pt. Subsequent sulfation of this catalyst produced sample marked TiO_2-Pt-S. Platinum deposition was performed according to the following method. 1 g of TiO_2 suspended in 20 ml of water was poured into a 50 ml beaker under stirring. Then 0.2 ml of 0.257 M H_2PtCl_6 stabilized with 0.05 M HCl was added. The Pt reduction was conducted by the dropwise addition of the 3-fold molar excess of a cold $NaBH_4$ water solution. In our case it was 2 ml of 3 mg/ml $NaBH_4$ solution. The obtained precursor was washed 3 times with water and dried at 120 °C. The second step of preparation, sulfation, was identical to that for TiO_2-S sample.

Specific surface area, platinum and sulfur content were measured by the low temperature nitrogen adsorption (ASAP 2400, USA) and by X-ray fluorescence analysis with VRA-20 instrument correspondingly. The results are summarized in Table 1.

Using the fact that Pt deposition does not influence the specific surface area [30] one can conclude from the data in Table 1 that it does not depend on the TiO_2 treatment in the present work and equals to about 340 m^2/g for all the samples.

TEM images were obtained with a JEM-2010 transmission electron microscope to describe the TiO_2, TiO_2-S and TiO_2-Pt-S samples.

2.2. Surface titration and CO adsorption methods

Surface titration method used in this work is based on the adsorption of organic acids and bases on the catalyst surface from anhydrous *n*-heptane (reference grade) solution [17]. Measurements of the probe species concentration in *n*-heptane solution were performed by a Perkin Elmer Lambda 35 UV/VIS spectrophotometer. The chemical formula, strength and spectroscopic data of the used probe species are presented in Table 2.

Table 2
Thermodynamic and spectroscopic data on the probe species used in the surface titration experiments

Probe species	Strength, pK	λ_{max}, nm	Absorption coefficient $\varepsilon \times 10^{-3}$, L/(mol cm)
Acids			
Benzoic acid, $C_7H_6O_2$	$pK_a = 4.2$	230	11.5
o-Nitrophenol, $C_6H_4(NO_2)(OH)$	$pK_a = 7.17$	270	6.81
Bases			
Piperidine, $C_5H_{11}N$	$pK_b = 2.88$	211	0.975
Pyridine, C_5H_5N	$pK_b = 8.77$	251	1.72
o-Fluoroaniline, C_6H_6FN	$pK_b = 10.8$	230	9.06
Diphenylamine, $C_{12}H_{11}N$	$pK_b = 13.2$	282	16.1

Benzoic acid was preliminary purified via the double recrystallization whereas *o*-nitrophenol (Acros organics 99%), piperidine (analytical grade), pyridine (analytical grade), *o*-fluoroaniline (Acros organics 99+%) and diphenylamine (high-purity grade) were used as supplied.

Further, 2×10^{-3} M solutions of these substances in heptane were prepared. 3 mg portions of catalyst samples under study were placed into the flasks with ground stoppers, and 5 ml solution of probe species were added. By measuring absorbance of the solutions before and after their contact with TiO_2 one can estimate the quantity of probe molecules adsorbed and consequently the number of appropriate surface sites according to the formula

$$\nu_{ads} = \frac{D_0 - D}{\varepsilon \cdot l \cdot m} \cdot V, \quad (1)$$

where D_0 and D are the absorbance of the solutions before and after their contact with TiO_2 (dimensionless), V is the solution volume (L), l is the cell path length (cm), ε is the absorption coefficient (L/(cm mol)), m is the catalyst mass (g).

A low temperature CO adsorption was studied for the TiO_2 and TiO_2-S samples which were pressed into the tablets with 10–15 mg/cm^2 density. Prior to the CO adsorption, the tablets were treated in vacuum at 150 °C for 90 min. The Bruker Vector 22 FT-IR spectrometer with 2 cm^{-1} resolution and 32 scans accumulation regime was used for spectra recording.

2.3. Acetone photocatalytic oxidation

Kinetic measurements were conducted in the flow-circulating system described in detail elsewhere [30,31]. This system includes a quartz reactor thermostated at 40 °C, a membrane circulation pump and a gas module connected with a stainless steel pipes.

Photocatalyst samples were uniformly deposited onto the 3 × 3 cm glass support from aqueous suspension with subsequent drying at room temperature. The density of obtained samples (3 mg/cm^2) guaranteed the complete absorption of incident light from a 1000 W high-pressure Xe lamp. The lamp irradiation was preliminary transmitted through water and 313-nm interference filters. The UV irradiance was 7 mW/cm^2.

Input gas mixture consisted from air, water vapor (4500 ± 500 ppm) and acetone vapor (varying from 0 to 6000 ppm). The input and output (after flow-circulating system) gas mixtures were analyzed for the water, acetone and CO_2 content with gas chromatographs equipped with FID and TCD detectors.

The rate of acetone oxidation W_{ox} (mol/s) was calculated from the difference between CO_2 concentrations in the output and input gas mixtures after the steady state was reached according to the following formula:

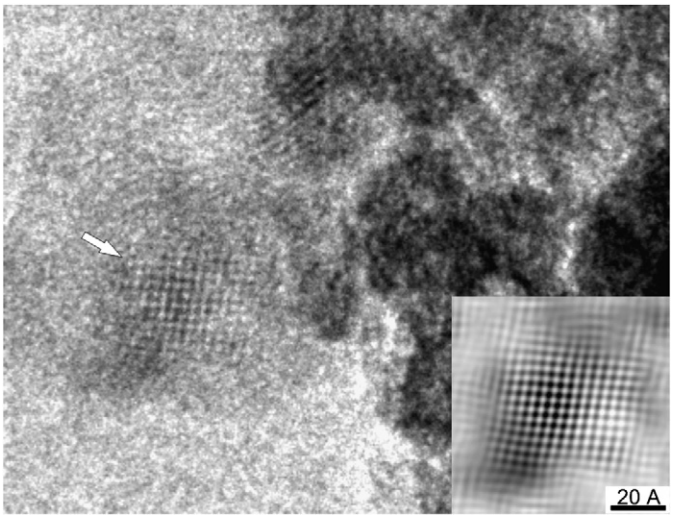

Fig. 1. TEM image of TiO_2 Hombifine N.

$$W_{ox} = \frac{\Delta C \cdot u \cdot 10^{-9}}{3 \cdot R \cdot T}, \quad (2)$$

where ΔC (ppm) $= C_{out} - C_{in}$ is the difference between CO_2 concentrations in the output and input gas; u (cm^3/s) is the gas flow through the flow-circulating system; $R = 0.082$ (L atm)/(mol K); T (K) is the temperature. In the present work $u = 0.58$–0.6 cm^3/s, $T = 313$ K, ΔC varied from 0 to 500 ppm. Formula (2) uses the fact that one acetone molecule transforms into the three CO_2 molecules during the photocatalytic oxidation and it was controlled at each steady state point by mass balance calculations. It means that no other carbon-containing species except the acetone and CO_2 were detected during the experiments and the ratio $\Delta C_{CO_2}/\Delta C_{ac}$ was practically equal to 3, where ΔC_{CO_2} and ΔC_{ac} are the differences of the inlet and outlet concentrations of CO_2 and acetone correspondingly. The preference of using the ΔC_{CO_2} instead of the directly measuring ΔC_{ac} value in the formula (2) is explained by the fact that at a high acetone concentration the values of ΔC_{ac} become small compared with the absolute inlet acetone concentration. At the same time, the inlet CO_2 concentrations in our experiments was equal to 0 so the ΔC_{CO_2} was equal to outlet CO_2 concentration. In this way, the precision of the ΔC_{CO_2} value was noticeably better than for ΔC_{ac}.

3. Results and discussion

3.1. Surface investigation

High resolution TEM images of unmodified TiO_2, modified with sulphuric acid (TiO_2-S) and with Pt and H_2SO_4 (TiO_2-Pt-S) are presented in Figs. 1–3, respectively. All samples are relatively transparent. Therefore images contrast was enhanced for the better view.

The initial TiO_2 consists of primary particles with the size of ≈5 nm, which are agglomerated into secondary particles of 500–1000 nm diameter. The surface of particles is not clearly defined. The arrow in Fig. 1 shows a single anatase particle with the well defined lattice. The same particle is shown in the lower right part of Fig. 1 after the Fourier filtration. The observed interfacial distance in the lattice is equal to 3.6 Å and the rows are situated at the right angle to each other. The distance coincides well with the lattice constant of anatase $a = b = 3.733$ Å. Therefore, the observed particle face is believed to correspond to the (001) surface of anatase [32].

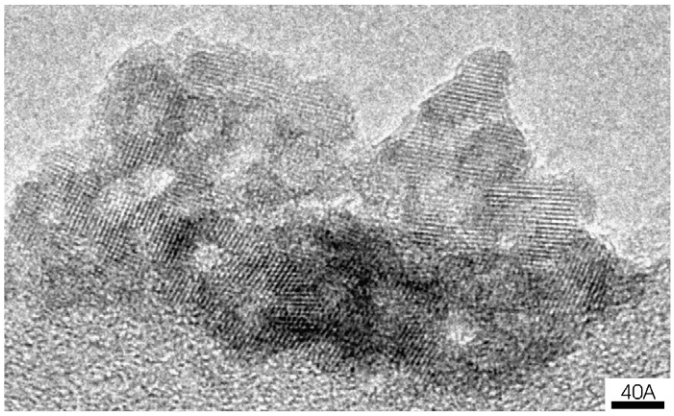

Fig. 2. TEM image of TiO_2-S sample. A thin amorphous layer of about 3 Å thickness covers the catalyst surface.

After sulfation under mild conditions, the TiO_2 particles surface underwent significant changes. Surface of the particles is more clearly defined. The main difference in the TiO_2-S sample shown in Fig. 2 is that one can observe a thin amorphous layer of about 3 Å thickness covering the sample surface. A similar layer was also observed over the surface of sulfated platinized sample TiO_2-Pt-S (Fig. 3A). This layer was completely absent in the unmodified initial TiO_2 (Fig. 1). The Pt particle in TiO_2-Pt-S catalyst is shown in Fig. 3B.

Although the noticeable dissolution of TiO_2 on macroscopic scale occurs only in hot concentrated sulfuric acid [33], interaction with 4 M H_2SO_4 can result in slight surface dissolution. Mogyorosi with co-workers [34] obtained titanium dioxide samples that contained 72.4 wt% anatase and 27.6 wt% amorphous phase by the sol–gel method in an acidic environment. In [35] the authors reported that amorphous oxo phase of titanium oxide exhibits considerable activity toward photocatalytic degradation of trichloroethylene in the gas phase.

If one calculates the surface sulfur concentration from the data presented in Table 1 it will be equal to about 0.8 atom/nm^2, i.e. approximately one sulfur atom or SO_4^{2-} group per one surface Ti atom. Therefore a thin amorphous layer in our case could be the surface sulfates or the thin $TiO(SO_4)$ film.

The diameter of Pt particles over the TiO_2-Pt-S surface was in the range of 1.5–2 nm (Fig. 3B). The calculation of sample surface area occupied by Pt particles based on the total Pt content given in Table 1 provides the value of approximately 0.33–0.44 m^2 per g of the sample. Only a very small portion of the total TiO_2 surface is covered with platinum particles. This agrees well with previous characterizations of Pt-containing TiO_2 of analogous Pt content [27].

Fig. 3. TEM images of sample TiO_2-Pt-S. (A) A thin amorphous layer of about 3 Å thickness can be observed on the surface; (B) the arrow shows the Pt particle. The same particle is shown in the bottom left part of the image after the Fourier filtration. The observed interfacial distance in the metal lattice is equal to 2.3 Å.

3.2. CO adsorption and surface titration

IR spectra of TiO_2 and TiO_2-S samples treated in vacuum at 150 °C before CO adsorption are shown in Fig. 4. 1235 and 1333 cm^{-1} absorption bands appeared after the surface sulfation (spectrum b). The 1333 cm^{-1} band is close to the stretching frequency of S=O and the 1200–1250 cm^{-1} band is close to the characteristic frequencies of SO_4^{2-} [10] with a lower symmetry C_{3v} or C_{2v} corresponding to mono- and bidentate sulfates [36].

The adsorption of aliquots of CO gives rise to absorption band situated at about 2190 cm^{-1} and appearance of absorption band at 2160 cm^{-1} at high CO pressure (40 Torr) (Fig. 5). The first type of absorption band corresponds to CO adsorbed on the surface Ti^{4+} centers of TiO_2 [37,38]. This band has a gradual shift of its maximum to the lower frequencies (wavenumbers) with the growth of the amount of adsorbed CO. The position of this band is supposed to be the indicator of the strength of surface acidic sites. The stronger shift of this band to the higher wavenumbers relatively to the valence absorption band of gaseous CO (2143 cm^{-1} [36]) corresponds to the stronger CO interaction with the surface centers and, therefore, such centers are stronger Lewis acids. Moreover, using the absorption band areas one can estimate the relative or absolute concentrations of surface Lewis sites according to the modified law of absorbance in the form

$$A = A_0 \cdot d \cdot C, \tag{3}$$

where A is the absorption band area (cm^{-1}), A_0 is the CO absorbance coefficient for the particular adsorbent and wavenumber

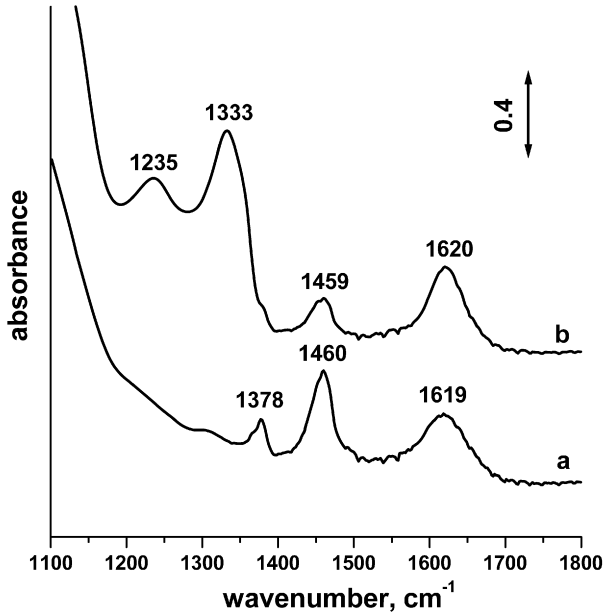

Fig. 4. FTIR spectra of TiO_2 (a) and TiO_2-S (b) samples treated in vacuum at 150 °C for 90 min. Tablet densities were 15.3 and 11.3 mg/cm^2 for TiO_2 and TiO_2-S samples, respectively.

(cm/μmol), d is the tablet density (mg/cm^2) and C is the surface sites concentration (mmol/g) [17].

In this way, the surface sites of TiO_2-S sample are more acidic than those of unmodified TiO_2 since their value of $\Delta\nu$(CO) shift to the higher frequency is 3 to 5 cm^{-1} higher for TiO_2-S sample than for pure unmodified TiO_2 (Fig. 5). The difference of CO heats of adsorption for these two samples could be estimated from the following correlation reported by Zaki [39]:

$$\Delta H_{ads}(CO) = 10.5 + 0.5 \cdot \Delta\nu(CO)\ \text{kJ mol}^{-1}. \quad (4)$$

The difference ΔH_{ads}(CO) for TiO_2 and TiO_2-S samples is in the range of 1.5–2.5 kJ mol^{-1} indicating that sites strength difference is noticeable but not high.

The ratio of Ti^{4+} Lewis sites quantity over sulfated and unsulfated samples derived from the absorbance law varies from 1.4 to 1.6 for the first–third spectra (Figs. 5A and 5B) indicating that the concentration of Lewis sites on the surface of TiO_2-S sample is about 1.5 times higher.

2157 and 2160 cm^{-1} adsorption bands (Fig. 5) correspond to physically adsorbed or H-bonded CO [39] since the corresponding surface OH group valence bands in the 3670–3730 cm^{-1} region are decreased and shifted to the lower wavenumbers of 3500–3600 cm^{-1} (Figs. 6A and 6B) during the CO adsorption. The total change of IR spectra of TiO_2 and TiO_2-S samples during the CO adsorption was barely visible. Therefore the resulting IR spectra change in Fig. 6 is represented in the differential form with the subtracted IR spectrum of TiO_2 and TiO_2-S samples taken before CO adsorption.

In this case one could see that at least 3 types of OH-group vibrations disappear upon CO adsorption on the unmodified TiO_2 sample (Fig. 6A)—3670, 3690 and 3714 cm^{-1} adsorption bands; only 2 types of OH-groups vibration bands (Fig. 6B)—3674 and 3713 cm^{-1}—decrease upon CO adsorption on the surface of TiO_2-S sample. It means that, probably, two types of surface OH-groups of pure TiO_2 corresponding to 3670 and 3690 cm^{-1} bands were converted into a one type surface OH-groups for the TiO_2-S sample corresponding to 3674 cm^{-1} band during the sample sulfation. In other words, it is possible that there is adsorption of SO_4^{2-} ions in the mono- or bidentate forms by the interaction with terminal and

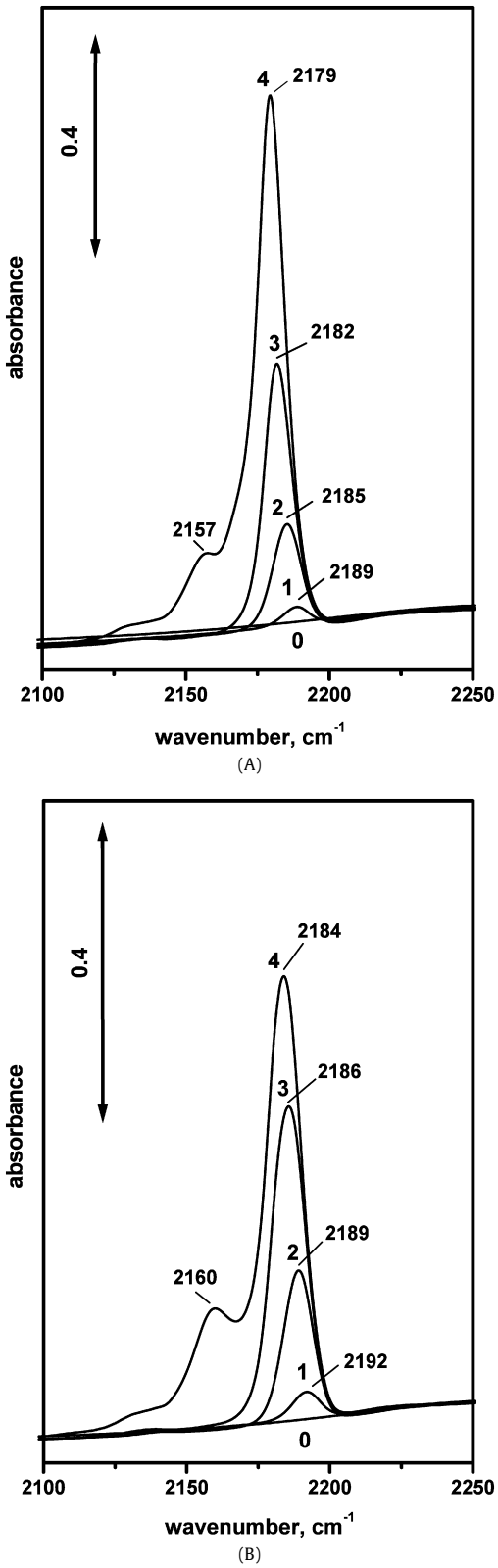

Fig. 5. IR spectra of catalysts during low temperature CO adsorption: (A) TiO_2, (B) TiO_2-S. Numerals above the spectra correspond to CO pressure: (0) no CO admission; (1) 3 Torr; (2) 11 Torr; (3) 21 Torr; (4) 40 Torr. Tablets densities were 15.3 and 11.3 mg/cm^2 for the TiO_2 and TiO_2-S samples, respectively.

bridge OH-groups that converts them into the one type of S atom bonded OH-groups.

Another very powerful method to study acid–base surface sites is adsorption of probe molecules from solutes [40,41]. Results of

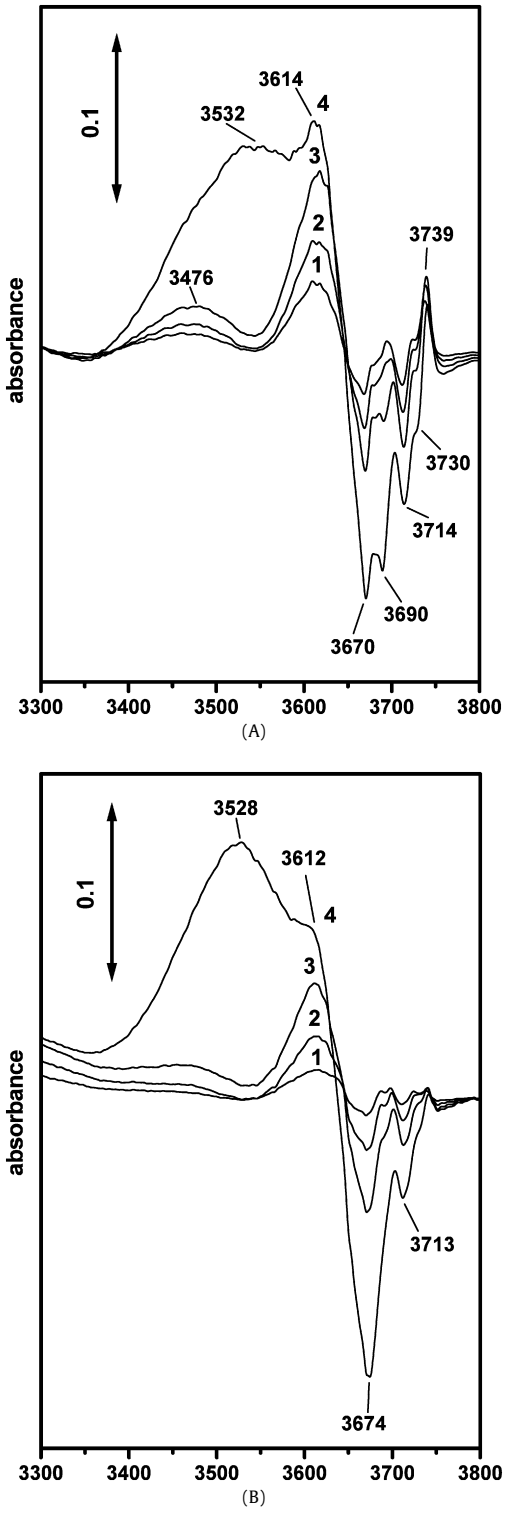

Fig. 6. Changes of IR spectra of TiO_2 (A) and TiO_2-S (B) in the valence OH vibrations region during the CO adsorption. All the spectra are the result of subtraction of the initial spectrum of the samples before CO adsorption.

the TiO_2, TiO_2-S and TiO_2-Pt-S samples titration by probe organic species are presented in Table 3. In our previous research [17] only one type of organic base and acid was used for titration giving the correlation of activity with the total quantity of surface acidic and basic sites. An attempt to classify the range of acidic sites by their strength is done in the present work.

The strongest species—benzoic acid ($pK_a = 4.2$) and base piperidine ($pK_b = 2.88$)—should adsorb on a variety of basic and acidic sites, respectively, giving the highest quantity of adsorbed probe species for all the three studied samples (Table 3). At the same time, the weakest acid, *o*-nitrophenol ($pK_a = 7.17$), and base, diphenylamine ($pK_b = 13.2$), should adsorb only on relatively strong basic and acidic sites giving the lowest quantity of adsorbed species. In this assumption we have neglected the possible specific adsorption of some of the probe species which was not investigated in this work. One should keep in mind that specific adsorption can result in an over-estimation of surface sites quantity compared with the actual one.

Table 3
Quantity of adsorbed probe species on the surface of TiO_2, TiO_2-S and TiO_2-Pt-S samples

Probe species	Strength, p*K*	Adsorbed quantity, mmol/g (molecules/nm^2)		
		TiO_2	TiO_2-S	TiO_2-Pt-S
Acids				
Benzoic acid	$pK_a = 4.2$	1.25 (2.2)	0.96 (1.7)	0.66 (1.2)
o-Nitrophenol	$pK_a = 7.17$	0.60 (1.1)	0.27 (0.5)	0.08 (0.1)
Bases				
Piperidine	$pK_b = 2.88$	0.85 (1.5)	1.13 (2)	0.77 (1.4)
Pyridine	$pK_b = 8.77$	0.67 (1.2)	0.72 (1.3)	0.47 (0.8)
o-Fluoroaniline	$pK_b = 10.8$	0.23 (0.4)	0.50 (0.9)	0.24 (0.4)
Diphenylamine	$pK_b = 13.2$	0.16 (0.3)	0.28 (0.5)	0.20 (0.35)

Colon with co-workers [9] estimated the total quantity of acid sites on the surface of sulfated TiO_2 to be equal to 1 μmol/m^2 by the microcalorimetric pyridine adsorption. The highest concentration for TiO_2-S sample (Table 3) is equal to 1.13 mmol/g or 3.3 μmol/m^2 although the SO_4^{2-} species surface concentration is even higher in our case. Thus, the mild sulfation technique produces higher surface concentration of acidic groups.

The comparison of adsorption data for pure TiO_2 and TiO_2-S samples (Table 3) shows that quantity of basic sites (total and only strong) decrease after the H_2SO_4 treatment. At the same time, quantities of acidic sites are increased including the most strong ones measured by diphenylamine titration. The ratio of acidic sites quantities for TiO_2-S and TiO_2 samples is equal to 1.33, 1.07, 2.17 and 1.75 for piperidine, pyridine, *o*-fluoroaniline and diphenylamine, respectively, and is in satisfactory agreement with the CO absorption band intensities ratio which is equal to about 1.5. Therefore, both methods give the correlating results about quantity and strength of acidic centers.

The quantity of strong acidic sites on the surface of platinized TiO_2-Pt-S sample is equal to 0.2 mmol/g and is also greater than for pure TiO_2 sample. At the same time, the total acidity measured by piperidine adsorption is the lowest among the three studied samples (Table 3). The quantity of basic sites over TiO_2-Pt-S sample is two-fold lower than for initial TiO_2 and about 1.5-fold lower than for sulfated TiO_2. Such a decrease in acid and base sites quantity in TiO_2-Pt-S is unexpected and cannot be explained by surface blocking by Pt particles since their surface was estimated above and is equal to just 0.33–0.44 m^2/g. Moreover, in the next section it will be demonstrated that TiO_2-Pt-S sample possesses the highest photoactivity.

In our previous work [30] it was shown that treatment of TiO_2 with $NaBH_4$ which we are using for Pt reduction even without additions of H_2PtCl_6 resulted in significant changes of catalytic properties. Namely, the treated catalyst possessed lower activity in the low temperature range but higher activity at elevated temperatures and higher stability toward thermal deactivation in acetone photocatalytic oxidation. Adsorbed boron species probably in the form of borates can effectively block the Ti^{4+} surface species that are responsible for surface acidic sites. That is why in the kinetic experiments we additionally investigated TiO_2 with 1% of deposited Pt but without further acidic treatment (marked as TiO_2-Pt) to elucidate the effect of sulfation on the photooxidation rate.

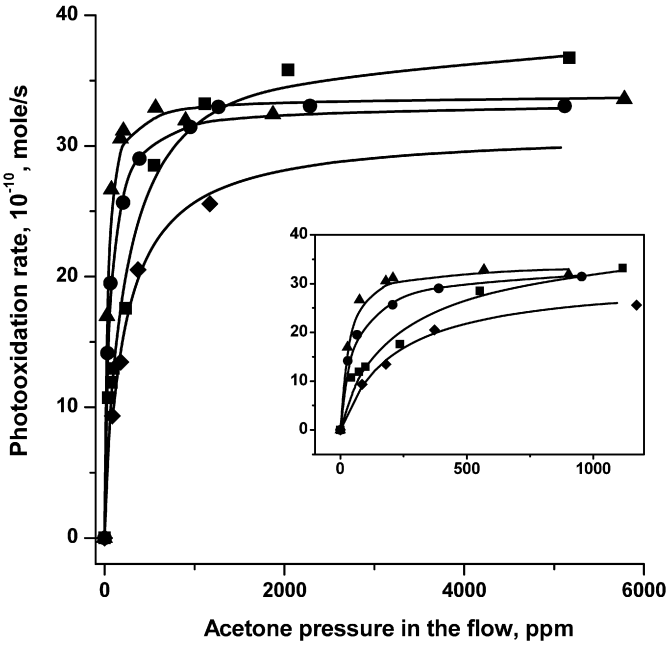

Fig. 7. Steady-state acetone photocatalytic oxidation rate as a function of its concentration in the flow-circulating reactor for different photocatalysts: (■) TiO_2; (●) TiO_2-S and (▲) TiO_2-Pt-S, (◆) TiO_2-Pt. In the inset is shown the region of small concentrations.

3.3. Kinetics of acetone vapor photocatalytic oxidation

The dependence of the steady-state rates of the acetone vapor photocatalytic oxidation on its concentration for TiO_2, TiO_2-S, TiO_2-Pt-S and TiO_2-Pt samples is shown in Fig. 7. All the data points are well described by the one adsorption site Langmuir–Hinshelwood equation:

$$W_{OX} = \frac{k_r \cdot K_{ads} \cdot C}{1 + K_{ads} \cdot C}, \quad (5)$$

where k_r and K_{ads} are the photooxidation rate and acetone adsorption constants; C is the acetone gas phase concentration. Constant k_r in this equation also could be considered as the maximum photooxidation rate at high acetone concentration ($K_{ads} \cdot C \gg 1$). Solid curves shown in Fig. 7 are the result of approximation of experimental data. Calculated values of k_r and K_{ads} are listed in Table 4.

Constant k_r is equal to 33×10^{-10} mol/s for TiO_2-Pt-S and TiO_2-S samples and is slightly higher (38×10^{-10} mol/s) and slightly lower (31×10^{-10} mol/s) for pure TiO_2 and TiO_2-Pt samples, correspondingly. The curves in Fig. 7 show that at acetone concentration above 1500 ppm, unmodified TiO_2 possesses the highest oxidation rate that is connected with the highest rate constant for this sample whereas TiO_2-Pt demonstrates the lowest oxidation rate that we believe is associated with partial blocking of TiO_2 surface with boron species produced from the $NaBH_4$ treatment.

In general, at high acetone concentration levels (>1500 ppm) all samples have similar photocatalytic activity because the acetone monolayer formation has been completed on samples surfaces. Under these conditions the value of adsorption constant K_{ads} does not play any significant role and activity is determined by the quantity of active sites and turnover rate. The quantity of active sites can be estimated as equal if one takes it proportional to the surface area, which in turn is similar for all samples. Thus, turnover rate is also similar for all the catalysts. This means that the electron–hole separation is also similar for sulfated and untreated samples in contrast to hypothesis of works [12,13].

In many cases contaminants concentrations are low and are not enough for significant surface coverage of photocatalyst. Under such conditions, the adsorption characteristics of the photo(catalyst) have the critical importance. This situation corresponds to the low acetone concentration level (<500 ppm).

Table 4
Results of approximation of acetone photocatalytic oxidation by the Langmuir–Hinshelwood model (5)

Sample	k_r, 10^{-10}, mol/s	K_{ads}, ppm^{-1}
1% Pt/TiO_2 (unsulfated)	31.13 ± 0.5	$4.7 \times 10^{-3} \pm 3.8 \times 10^{-4}$
TiO_2	38.3 ± 1.5	$5.3 \times 10^{-3} \pm 8.3 \times 10^{-4}$
TiO_2-S	33.2 ± 0.4	$2.2 \times 10^{-2} \pm 1.8 \times 10^{-3}$
TiO_2-Pt-S	33.8 ± 0.5	$4.1 \times 10^{-2} \pm 4.4 \times 10^{-3}$

The inset in Fig. 7 shows the photocatalytic oxidation rates in this low concentration range. The TiO_2-Pt catalyst is still the least active sample. Pure TiO_2 sample has a bit higher rate of photooxidation. The sulfated TiO_2-S sample has intermediate activity and the highest activity is demonstrated by the platinized and sulfated TiO_2-Pt-S sample. For example, at the acetone concentration level near 150 ppm the PCO rate close to 13, 16, 24 and 29×10^{-10} mol/s values for TiO_2-Pt, TiO_2, TiO_2-S and TiO_2-Pt-S samples, respectively. Moreover, at the lower acetone concentration levels this difference will be even higher indicating that in such low concentration conditions the sulfated and especially sulfated platinized TiO_2 samples work more than 3 times effectively.

Here we have to discuss two moments. On the one hand, there is the dramatic increase of adsorption properties of platinized TiO_2 treated with sulphuric acid (TiO_2-Pt-S) against the untreated one. Indeed, the sulfation procedure increased the K_{ads} by an order of magnitude from 0.0047 to 0.041 ppm^{-1}. The absolutely similar sulfation procedure in the case of non-platinized TiO_2 resulted in only 4 time increase of K_{ads} from 0.0053 to 0.022 ppm^{-1} value. The stronger influence of sulfation procedure on the photoactivity of Pt-loaded TiO_2 samples probably could be explained by the removal of oxygen containing boron species from TiO_2 surface. Such species could form as a result of $NaBH_4$ oxidation with H_2PtCl_6 during the chemical deposition procedure.

On the other hand, there is not a big difference in adsorption constant between Hombifine TiO_2 and its platinized form TiO_2-Pt but more than two-fold increase in adsorption constant for TiO_2-Pt-S as compared to TiO_2-S samples. We attribute this behavior to the suppressing influence of Pt-deposition procedure which produces the oxygen containing boron species on the TiO_2 surface. In fact, in the case of TiO_2 and TiO_2-Pt samples, the possible positive effect of Pt deposition was suppressed by the adsorbed boron species unlike the case of TiO_2-S and TiO_2-Pt-S samples where the sulfation procedure after the Pt-deposition washed out the boron species. Two additional observations support this assumption:

(1) A ^{11}B NMR signal was observed in the TiO_2-Pt sample corresponding to the 0.012 wt% of tetrahedral BO_4 species. And this signal was not observed in the TiO_2-Pt-S sample giving us an idea that it was simply washed out during the sulfation procedure.
(2) The sample prepared by the reverse sequence, i.e. Pt deposition was done after the sulfation procedure (TiO_2-S-Pt), demonstrated a lower photocatalytic activity than TiO_2-Pt-S sample but still higher than untreated and platinized TiO_2 and TiO_2-Pt samples in the flow-circulating system at the 500 ppm acetone vapor pressure. It means that there are remaining boron species on the surface of TiO_2-S-Pt sample suppressing its photoactivity just because the Pt-deposition procedure was the last.

Based upon the data above we could say that in any case the sulfation procedure makes the more pronounced effect on the TiO_2

photoactivity against VOC's PCO unlike the Pt chemical deposition based on the H_2PtCl_6 reduction with $NaBH_4$.

Most probably, an additional study of the surface state before and after the reaction would expand our understanding of the origin of high photocatalytic activity at the low acetone concentration level. In our opinion such investigations should include comparative FTIR reflectance spectroscopy of TiO_2 surface in the course of prolonged PCO experiments to accumulate the surface changes.

4. Conclusions

Low temperature CO adsorption and titration with dissolved organic probe species were used for characterization of surface acid and base sites of pure and sulfated TiO_2 catalyst. The agreeing results indicate that the quantity and strength of surface acid sites increases as a result of this treatment. Deposition of platinum and sulfation decreases the number of surface acid and base sites compared to sulfated TiO_2.

The dependence of steady-state rate of acetone vapor photocatalytic oxidation for TiO_2, SO_4^{2-}/TiO_2, (1% Pt)/TiO_2 and (1% Pt, SO_4^{2-})/TiO_2 samples obeys the Langmuir–Hinshelwood kinetic model. All samples have a similar activity in the high acetone concentration range that signifies the completion of acetone monolayer coverage on the surface.

In the low concentration range, the more acidic sulfated TiO_2 possesses a higher photocatalytic activity due to the increase of acetone adsorption constant which correlates with the surface acidity according to CO and organic probe species adsorption data.

The highest photoactivity of (1% Pt, SO_4^{2-})/TiO_2 sample can be explained by cumulative effect of platinum and SO_4^{2-} addition on acetone adsorption constant.

Acknowledgments

Support by NATO SfP-981461 and ISTC 3305 grants is gratefully acknowledged. One of the authors (D.V.K.) appreciates the support of the “Russian Science Support Foundation.”

References

[1] A.H. Boonstra, A.H.A. Mutsaers, J. Phys. Chem. 79 (1975) 1694.
[2] G. Munuera, V. Rives-Arnau, A. Saucedo, J. Chem. Soc. Faraday Trans. 1 75 (1979) 736.
[3] J. Papp, S. Soled, K. Dwight, A. Wold, Chem. Mater. 6 (1994) 496.
[4] T. Yamaguchi, Y. Tanaka, K. Tanabe, J. Catal. 65 (1980) 442.
[5] Y.T. Kwon, K.Y. Song, W.I. Lee, G.J. Choi, Y.R. Do, J. Catal. 191 (2000) 192.
[6] T. Kantoh, S. Okazaki, Bull. Chem. Soc. Jpn. 54 (1981) 3259.
[7] X.Y. Deng, Y.H. Yue, Z. Gao, Appl. Catal. B 39 (2002) 135.
[8] G. Colon, M.C. Hidalgo, J.A. Navio, Appl. Catal. B 45 (2003) 39.
[9] G. Colon, M.C. Hidalgo, G. Munuera, I. Ferino, M.G. Cutrufello, J.A. Navio, Appl. Catal. B 63 (2006) 45.
[10] M.C. Hidalgo, M. Maicu, J.A. Navío, G. Colón, Appl. Catal. B 81 (2008) 49–55.
[11] S.K. Samantaray, P. Mohapatra, K. Parida, J. Mol. Catal. A 198 (2003) 277.
[12] N. Keller, E. Barraud, F. Bosc, D. Edvards, V. Keller, Appl. Catal. B 70 (2007) 423.
[13] E. Barraud, F. Bosc, D. Edvards, N. Keller, V. Keller, J. Catal. 235 (2005) 318.
[14] D.S. Muggli, L. Ding, Appl. Catal. B 32 (2001) 181.
[15] J.C. Yu, J.G. Yu, J.C. Zhao, Appl. Catal. B 36 (2002) 31.
[16] D.V. Kozlov, E.A. Paukshtis, E.N. Savinov, Appl. Catal. B 24 (2000) L7.
[17] D. Kozlov, D. Bavykin, E. Savinov, Catal. Lett. 86 (2003) 169.
[18] D.V. Kozlov, A.A. Panchenko, D.V. Bavykin, E.N. Savinov, P.G. Smirniotis, Russian Chem. Bull. 52 (2003) 1100.
[19] A. Mills, S.L. Hunte, J. Photochem. Photobiol. A Chem. 108 (1997) 1.
[20] E. Kowalska, H. Remita, C. Colbeau-Justin, J. Hupka, J. Belloni, J. Phys. Chem. C 112 (2008) 1124.
[21] Y. Ishibai, J. Sato, T. Nishikawa, S. Miyagishi, Appl. Catal. B 79 (2008) 117.
[22] M. Fernandez-Garcia, A. Fuerte, M.D. Hernandez-Alonso, J. Soria, A. Martinez-Arias, J. Catal. 245 (2007) 84.
[23] W.Y. Teoh, L. Madler, R. Amal, J. Catal. 251 (2007) 271.
[24] E.A. Kozlova, A.V. Vorontsov, Appl. Catal. B 77 (2007) 35.
[25] Z.B. Lei, G.J. Ma, M.Y. Liu, W.S. You, H.J. Yan, G.P. Wu, T. Takata, M. Hara, K. Domen, C. Li, J. Catal. 237 (2006) 322.
[26] S. Higashimoto, K. Takamatsu, M. Azuma, M. Kitano, M. Matsuoka, M. Anpo, Catal. Lett. 122 (2008) 33.
[27] B. Sun, A.V. Vorontsov, P.G. Smirniotis, Langmuir 19 (2003) 3151.
[28] M. Ikeda, Y. Kusumoto, Y. Yakushijin, S. Somekawa, P. Ngweniform, B. Ahmmad, Catal. Commun. 8 (2007) 1943.
[29] A.V. Vorontsov, V.P. Dubovitskaya, J. Catal. 221 (2004) 102.
[30] A.V. Vorontsov, I.V. Stoyanova, D.V. Kozlov, V.I. Simagina, E.N. Savinov, J. Catal. 189 (2000) 360.
[31] A.V. Vorontsov, E.N. Savinov, G.B. Barannik, V.N. Troitsky, V.N. Parmon, Catal. Today 39 (1997) 207.
[32] M. Horn, C.F. Schwerdtfeger, E.P. Meagher, Z. Kristallogr. 136 (1972) 273.
[33] C. Chambers, A.K. Holliday, Modern Inorganic Chemistry, Butterworth & Co., 1975.
[34] K. Mogyorosi, I. Dekany, J.H. Fendler, Langmuir 19 (2003) 2938.
[35] M. Benmami, K. Chhor, A.V. Kanaev, J. Phys. Chem. B 109 (2005) 19766.
[36] K. Nakamoto, Infrared and Raman Spectra of Inorganic and Coordination Compounds, fourth ed., Wiley, New York, 1986.
[37] K. Hadjiivanov, J. Lamotte, J.-C. Lavalley, Langmuir 13 (1997) 3374.
[38] B. Bonelli, M. Cozzolino, R. Tesser, M. Di Serio, M. Piumetti, E. Garrone, E. Santacesaria, J. Catal. 246 (2007) 293.
[39] M.I. Zaki, H. Knozinger, Spectrochim. Acta A 43 (1987) 1455.
[40] Y.J. Liu, E. Lotero, J.G. Goodwin, J. Catal. 242 (2006) 278.
[41] R.J. Chimentao, S. Abello, F. Medina, J. Llorca, J.E. Sueiras, Y. Cesteros, P. Salagre, J. Catal. 252 (2007) 249.